

Antiferromagnetic complexes with the metal–metal bond XXVIII¹. Synthesis and molecular structure of the antiferromagnetic cluster $[\text{CpCr}(\mu\text{-SCMe}_3)_2(\mu\text{-S})]_2(\mu_4\text{-S})[\text{PtMe}_3(\mu\text{-I})]_2$ ²

A.A. Pasynskii^{*}, Y.V. Torubaev, S.E. Nefedov, I.L. Eremenko, O.G. Ellert, V.K. Belsky,
A.I. Stastch

N.S. Kurnakov Institute of General and Inorganic Chemistry, Russian Academy of Sciences, 31 Leninsky Prosp. V-71, Moscow, Russia

Received 30 July 1996; accepted 22 August 1996

Abstract

The reaction of $[\text{CpCr}(\mu\text{-SCMe}_3)_2(\mu\text{-S})]$ (**1**) with $[\text{PtMe}_3\text{I}]_4$ in hot benzene leads to the formation of the tetranuclear cluster $[\text{CpCr}(\mu\text{-SCMe}_3)_2(\mu_4\text{-S})[\text{PtMe}_3(\mu\text{-I})]_2$ (**2**). According to X-ray data, cluster **2** contains a molecule of **1** (Cr–Cr 2.761(9) Å, Cr–S–Cr 70.1(4)°), coordinated to a diplatinum fragment via a $\mu_4\text{-S}$ atom (Pt–S 2.583(10) and 2.560(9) Å). **2** has antiferromagnetic properties ($-2J = 202 \text{ cm}^{-1}$) due to the interaction between two paramagnetic Cr(III) centers ($S = 3/2$). © 1997 Elsevier Science S.A.

Keywords: Platinum; Chromium; Sulfido; Antiferromagnetic behaviour; Crystal structure

1. Introduction

Application of the metal-containing fragments as ligands is an effective method of cluster design, particularly for the antiferromagnetic mixed-metal cluster syntheses using $[\text{CpCr}(\mu\text{-SCMe}_3)_2(\mu\text{-S})]$ (**1**) [1]. If the second element is the halogen-containing complex $[\text{LMX}]_2$, four processes can be observed:

(a) simple adduct formation [2], $[\text{ReNO}(\text{CO})_2\text{Cl}]_2(\mu\text{-Cl})_2 + \mathbf{1} \rightarrow [\text{CpCr}(\mu\text{-SCMe}_3)_2(\mu_3\text{-S})[\text{ReCl}_2\text{NO}(\text{CO})_2]]_2$;
(b) migration of the X atom from M to Cr leading to Cr–Cr bond cleavage [3], $\mathbf{1} + (\text{PPh}_3)_2\text{PdCl}_2 \rightarrow [\text{CpCrCl}(\mu\text{-SCMe}_3)_2(\mu_3\text{-S})[\text{PdPPh}_3]]_2$;

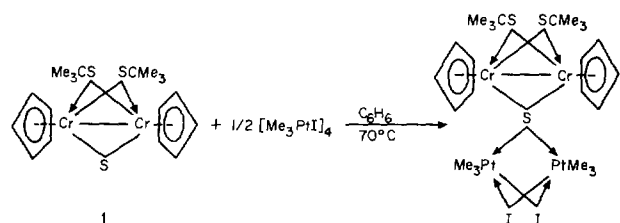
(c) elimination of the X atom and one of the CMe_3 groups with Cr–Cr bond retention [4], $\mathbf{1} + (\text{}^i\text{Pr}_3\text{P})_2\text{PdCl}_2 \rightarrow [\text{Cp}_2\text{Cr}_2(\mu\text{-SCMe}_3)(\mu_3\text{-S})_2[\text{Pd}(\text{}^i\text{Pr}_3\text{P})\text{Cl}]]_2$;

(d) migration of the X atom to Cr and CpCrCl₂ elimination (transmetallation reaction) [2], $[\text{CpCr}(\mu\text{-SCMe}_3)_2(\mu_3\text{-S})\text{ReCl}_2\text{NO}(\text{CO})_2] \rightarrow [\text{CpCrRe}(\text{NO})(\mu\text{-SCMe}_3)_2(\mu_3\text{-S})]_2$.

With this in mind, it was interesting to use the known $[\text{PtMe}_3\text{I}]_4$ complex [5] as a partner for **1**. This idea is based on the results of Abel et al. [6], who have used the Pt complex as initial for synthesis of a number of Me_3PtIL_2 complexes having sulfur-containing ligands.

2. Results and discussion

The interaction of **1** with $[\text{PtMe}_3\text{I}]_4$ in benzene at 70 °C results in a new tetranuclear cluster **2**:



2 was isolated as black crystals (from CH_2Cl_2) which are stable in air and moderately soluble in the usual

^{*} Corresponding author.

¹ For Part XXVII see Ref. [13].

² Dedicated to the memory of Professor Yu.T. Struchkov.

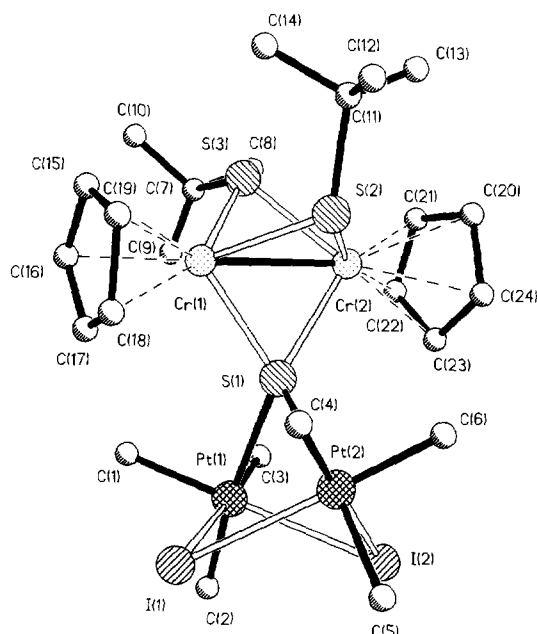


Fig. 1. Molecular structure of $[\text{CpCr}(\mu\text{-SCMe}_3)_2(\mu_4\text{-S})\text{PtMe}_3(\mu\text{-I})_2]$ (**2**).

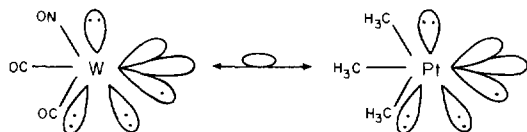
organic solvents. It is shown by X-ray analysis that **2** has a spirane-like structure with a central μ_4 -sulfur atom between Cr_2 and Pt_2 peripheral fragments (Fig. 1, Table 1). The first has practically linear $\text{Cp}_{\text{cent}}\text{Cr}-\text{CrCp}_{\text{cent}}$ system, and contains a direct $\text{Cr}-\text{Cr}$ bond (2.761(9) Å) supported by two SCMe_3 bridges (2.40(1) Å av.) and a μ_4 -S atom ($\text{Cr}-\text{S}$ 2.328(11) and 2.356(12) Å). The second has no $\text{Pt}-\text{Pt}$ bond, octahedrally coordinated Pt atoms are linked by two iodine bridges ($\text{Pt}-\text{I}$ 2.811(3), 2.835(3) Å) and one μ_4 -S atom ($\text{Pt}-\text{S}$ 2.583(10) and 2.560(9) Å). Each Pt atom has three methyl groups ($\text{Pt}-\text{C}$ 1.99(6) Å av.) in *facial* configuration

This structure is very similar to the arrangement of the recently studied $[\text{CpCr}(\mu\text{-SCMe}_3)_2](\mu_4\text{-S})[\text{W}(\text{CO})_2\text{NO}(\mu\text{-I})_2]$ (**3**) prepared from **1** and $\text{W}(\text{NO})(\text{CO})_4\text{I}$ [7]. **3** contains a direct $\text{Cr}-\text{Cr}$ bond (2.764(4) Å) in the Cr_2 fragment connected to the W_2 fragment via a μ_4 -S atom ($\text{Cr}-\text{S}$ 2.357(5), $\text{W}-\text{S}$ 2.551(1), 2.566(5) Å). No direct bond between W atoms is observed (μ_4 -S and μ -I bridges only) [7]. This is not surprising because of the isolobality of Me_3Pt and

Table 1
Main geometric parameters for cluster **2**

Bond	<i>d</i> (Å)	Bond	<i>d</i> (Å)	Bond	<i>d</i> (Å)
Pt(1)–I(1)	2.811(3)	Pt(1)–I(2)	2.835(3)	Pt(1)–S(1)	2.583(10)
Pt(1)–C(1)	1.909(60)	Pt(1)–C(2)	1.999(55)	Pt(1)–C(3)	2.063(31)
Pt(2)–I(1)	2.829(5)	Pt(2)–I(2)	2.843(3)	Pt(2)–S(1)	2.560(9)
Pt(2)–C(4)	2.048(57)	Pt(2)–C(5)	2.068(45)	Pt(2)–C(6)	2.035(32)
Cr(1)–Cr(2)	2.761(9)	Cr(1)–S(1)	2.328(11)	Cr(1)–S(2)	2.398(15)
Cr(1)–S(3)	2.337(16)	Cr(2)–S(1)	2.356(12)	Cr(2)–S(2)	2.411(15)
Cr(2)–S(3)	2.293(16)	S(2)–C(11)	1.850(45)	S(3)–C(7)	1.845(45)
Angle	ω (deg)	Angle	ω (deg)		
I(1)–Pt(1)–I(2)	86.6(1)	I(1)–Pt(1)–S(1)	82.1(2)		
I(2)–Pt(1)–S(1)	83.2(2)	I(1)–Pt(1)–C(1)	95.1(24)		
I(2)–Pt(1)–C(1)	178.2(26)	S(1)–Pt(1)–C(1)	96.5(16)		
I(1)–Pt(1)–C(2)	96.7(18)	I(2)–Pt(1)–C(2)	96.0(16)		
S(1)–Pt(1)–C(2)	178.5(11)	C(1)–Pt(1)–C(2)	84.4(22)		
I(1)–Pt(1)–C(3)	178.5(8)	I(2)–Pt(1)–C(3)	94.3(9)		
S(1)–Pt(1)–C(3)	96.8(10)	C(1)–Pt(1)–C(3)	84.0(26)		
C(2)–Pt(1)–C(3)	84.4(20)	I(1)–Pt(2)–I(2)	86.1(1)		
I(1)–Pt(2)–S(1)	82.1(2)	I(2)–Pt(2)–S(1)	83.4(2)		
I(1)–Pt(2)–C(4)	94.0(18)	I(2)–Pt(2)–C(4)	179.7(19)		
S(1)–Pt(2)–C(4)	96.3(14)	I(1)–Pt(2)–C(5)	90.4(15)		
I(2)–Pt(2)–C(5)	92.3(15)	S(1)–Pt(2)–C(5)	171.6(16)		
C(4)–Pt(2)–C(5)	88.0(20)	I(1)–Pt(2)–C(6)	177.3(9)		
I(2)–Pt(2)–C(6)	93.4(13)	S(1)–Pt(2)–C(6)	95.2(10)		
C(4)–Pt(2)–C(6)	86.5(22)	C(5)–Pt(2)–C(6)	92.3(18)		
Pt(1)–I(1)–Pt(2)	76.2(1)	Pt(1)–I(2)–Pt(2)	75.6(1)		
S(1)–Cr(1)–S(2)	81.4(4)	S(1)–Cr(1)–S(3)	99.9(5)		
S(2)–Cr(1)–S(3)	82.7(5)	S(1)–Cr(2)–S(2)	80.6(4)		
S(1)–Cr(2)–S(3)	100.3(5)	S(2)–Cr(2)–S(3)	83.4(5)		
Pt(1)–S(1)–Pt(2)	85.1(3)	Pt(1)–S(1)–Cr(1)	127.3(5)		
Pt(2)–S(1)–Cr(1)	124.2(4)	Pt(1)–S(1)–Cr(2)	129.2(4)		
Pt(2)–S(1)–Cr(2)	125.2(5)	Cr(1)–S(1)–Cr(2)	72.2(3)		
Cr(1)–S(2)–Cr(2)	70.1(4)	Cr(1)–S(3)–Cr(2)	73.2(5)		

W(NO)(CO)₂ moieties (d⁷-electron configuration) from the point of view of Hoffmann's definition [8]:



In both clusters, **2** and **3**, the Cr–Cr and Cr–(μ -S) bonds are elongated in comparison with **1** (Cr–Cr 2.689(8), Cr–S 2.24(1) Å) [9]. This difference is probably responsible for the decrease in exchange parameter ($-2J$) from 430 cm⁻¹ in **1** to 338 cm⁻¹ in **3** and 202 cm⁻¹ in **2** ($\mu_{\text{eff}} = 1.8(295 \text{ K}) - 0.8(79 \text{ K}) \mu_{\text{B}}$). Such an effect probably shows that a superexchange interaction over the μ_4 -S bridge plays a substantial role, along with direct interaction over metal–metal bonds. This fact is important to the understanding of the properties of chalcogen-containing MCr₂X₄ magnetic materials [10].

3. Experimental

All manipulations were carried out under argon. Solvents were dried and distilled before use. [PtMe₃I]₄ was prepared as described in Ref. [5] and [CpCr(μ -SCMe₃)₂(μ -S)]₂ as described in Ref. [9]. The IR spectra

Table 2
Crystallographic parameters, data collection and refinement for **2**

Number	2
Formula	C ₂₄ H ₄₆ Cr ₂ I ₂ Pt ₂ S ₃
Space group	<i>Pna</i> 2 ₁
<i>a</i> (Å)	19.671(4)
<i>b</i> (Å)	17.363(3)
<i>c</i> (Å)	9.903(2)
<i>V</i> (Å ³)	3382.3(17)
<i>Z</i>	4
ρ_{calc} (g cm ⁻³)	2.309
Absorb. coeff. μ (cm ⁻¹)	108.94
Radiation	Mo K α ($\lambda = 0.71073$ Å)
Scan type	θ -2 θ
Range 2 θ (deg)	2–52
Scan speed (deg min ⁻¹)	2.00–15.65
Index ranges	0 < <i>h</i> < 23, 0 < <i>k</i> < 20, 0 < <i>l</i> < 11
Independent reflections	3159
Observed reflections	
<i>I</i> > 4.0 σ	2450
Weighting scheme	Unit weights
Largest difference peak (e Å ⁻³)	3.39
Largest difference hole (e Å ⁻³)	-2.09
<i>R</i>	0.062
<i>R_w</i>	0.073

Table 3

Atomic coordinates ($\times 10^4$) and equivalent isotropic displacement coefficients (Å² $\times 10^3$)

Atom	<i>x</i>	<i>y</i>	<i>z</i>	<i>U_{eq}</i>
Pt(1)	2897(1)	3627(1)	1042	35(1)
Pt(2)	3312(1)	4667(1)	3930(3)	38(1)
I(1)	3623(2)	5019(2)	1211(4)	51(1)
I(2)	1996(1)	4268(2)	2973(4)	49(1)
Cr(1)	4708(3)	2790(4)	3206(7)	35(2)
Cr(2)	3587(3)	2194(4)	4522(8)	37(2)
S(1)	3615(4)	3303(5)	3152(10)	29(3)
S(2)	4511(6)	2873(8)	5591(13)	58(4)
S(3)	4449(8)	1492(8)	3564(15)	70(5)
C(1)	3493(27)	3166(53)	-246(44)	104(37)
C(2)	2342(26)	3907(37)	-575(56)	95(25)
C(3)	2388(16)	2591(18)	929(36)	28(10)
C(4)	4261(29)	4948(26)	4621(67)	75(24)
C(5)	3030(28)	5798(25)	4267(56)	66(20)
C(6)	3095(24)	4360(19)	5866(31)	42(14)
C(7)	4275(25)	816(24)	2169(44)	42(15)
C(8)	3837(38)	216(34)	2684(172)	256(82)
C(9)	3873(30)	1306(37)	1173(84)	106(27)
C(10)	4934(43)	612(34)	1791(87)	123(37)
C(11)	5108(22)	2347(26)	6700(42)	43(14)
C(12)	5379(39)	2940(52)	7670(69)	87(34)
C(13)	4751(37)	1829(33)	7677(63)	56(20)
C(14)	5737(38)	1981(55)	5974(74)	138(35)
C(15)	5773(38)	2848(83)	2821(116)	105(60)
C(16)	5381(28)	2680(26)	1408(41)	59(18)
C(17)	5145(27)	3429(36)	1449(47)	67(21)
C(18)	5236(48)	3776(48)	2387(106)	147(40)
C(19)	5513(68)	3629(73)	3133(87)	211(65)
C(20)	3069(28)	1674(42)	6416(46)	56(21)
C(21)	2950(43)	1155(38)	5234(110)	84(35)
C(22)	2667(43)	1489(42)	4203(67)	75(28)
C(23)	2464(25)	2268(46)	4730(69)	111(26)
C(24)	2784(44)	2337(49)	6054(116)	77(40)

Equivalent isotropic *U* defined as one third of the trace of the orthogonalized *U_{ij}* tensor.

were recorded on a Specord IR-75 in KBr pellets. Magnetic properties were studied by the Faraday method.

The crystal of **2** was mounted in air on a glass fiber using 5 min epoxy resin. The unit cell was determined and refined from 24 equivalent reflections with 23° < 2 θ < 26°, obtained from a CAD-4 four-circle diffractometer. The intensity data set was corrected for Lorentz and polarization effects. The DIFABS [11] method was used for absorption correction of **2** at the stage of an isotropic approximation. The background was scanned for 25% of the peak widths at each end of a scan. Three reflections were monitored periodically as a check for crystal decomposition or movement. No significant variation in these standards was observed; therefore, no correction was applied. Details of crystal parameters, data collection and structure refinement are given in Table 2.

The structure of **2** was solved using direct methods to locate all non-hydrogen atoms. After anisotropic refine-

ment, the H atoms of the Cp ligands and ¹Bu and Me groups were generated geometrically (C–H bonds fixed at 0.96 Å) and assigned the same isotropic temperature factor of $U = 0.08 \text{ \AA}^2$. Computations were performed using the SHELXTL PLUS program package [12] on a Pentium 4/80. The function minimized in the least-squares calculations was $\sum w(F_o - F_c)^2$. Atomic coordinates are listed in Table 3. Selected bond lengths and angles for **2** are given in Table 1. A complete list of bond lengths and angles and tables of anisotropic thermal parameters and hydrogen atom coordinates have been deposited at the Cambridge Crystallographic Data Centre.

3.1. Synthesis of $[\text{CpCr}(\mu\text{-SCMe}_3)_2(\mu_4\text{-S})[\text{PtMe}_3(\mu\text{-I})_2]$

A solution of 0.41 g (0.112 mmol) $[\text{PtMe}_3\text{I}]_4$ in hot benzene (5 ml) was added dropwise to an ink-violet solution of 0.25 g (0.56 mmol) $[\text{CpCr}(\mu\text{-SCMe}_3)_2(\mu\text{-S})]$ in 10 ml of benzene. The mixture was stirred at 70 °C for 1 h and then cooled to ambient temperature. The black precipitate formed was filtered off, washed with hexane (20 ml) and dried in vacuo. The filtrate was concentrated in vacuo, giving an additional quantity of black prisms. Yield 60%.

IR spectra (ν , cm^{-1}): 800 m, 810 s, 1000 m, 1130 m, 1430 m, 2900 m. Anal. Found: C, 25.3; H, 3.5. $\text{C}_{24}\text{H}_{46}\text{S}_3\text{Cr}_2\text{Pt}_2\text{I}_2$. Calc.: C, 24.4; H, 3.9%.

Monocrystals suitable for X-ray analysis were grown by slow evaporation of methylene chloride solution.

Acknowledgements

The authors are grateful to the Russian Foundation of Fundamental Research for financial support (Grants 96-03-33171 and 96-03-33172).

References

- [1] A.A. Pasynskii and I.L. Eremenko, *Uspekhi Khim.*, 58 (1989) 303.
- [2] I.L. Eremenko, H. Berke, B.I. Kolobkov and V.M. Novotortsev, *Organometallics*, 13 (1994) 244.
- [3] A.A. Pasynskii, I.L. Eremenko, G.Sh. Gasanov, O.G. Ellert, V.M. Novotortsev, Yu.V. Rakitin, T.Kh. Kurbanov, Yu.T. Struchkov and V.E. Shklover, *Polyhedron*, 3 (1984) 775.
- [4] I.L. Eremenko, V.M. Novotortsev, I.A. Petrunenko and H. Berke, *Izv. Akad. Nauk., Ser. Khim.*, (1995) 1334.
- [5] J.C. Baldwin and W.C. Kaska, *Inorg. Chem.*, 14 (1975) 2020.
- [6] E.W. Abel, I. Moss, K.G. Orrell, V. Sik, D. Stephenson, P.A. Bates and M.B. Hursthouse, *J. Chem. Soc., Dalton Trans.*, (1988) 521.
- [7] I.L. Eremenko, H. Berke, A.A. Van der Zeijen, B.I. Kolobkov and V.M. Novotortsev, *J. Organomet. Chem.*, 471 (1994) 123.
- [8] R. Hoffmann, *Angew. Chem., Int. Ed. Engl.*, 21 (1982) 711.
- [9] A.A. Pasynskii, I.L. Eremenko, Yu.V. Rakitin, V.M. Novotortsev, V.T. Kalinnikov, G.G. Aleksandrov and Yu.T. Struchkov, *J. Organomet. Chem.*, 165 (1979) 57.
- [10] T.I. Koneshova, K.V. Eremin and V.M. Novotortsev, *Neorg. Mater.*, 31 (1995) 1525.
- [11] N. Walker and D. Stuart, *Acta Crystallogr.*, A39 (1983) 158.
- [12] G.M. Sheldrick, in *Crystallographic Computing 3: Data Collection, Structure Determination, Proteins and DataBases*, Clarendon Press, New York, 1985, p. 175.
- [13] A.A. Pasynskii, I.L. Eremenko, S.E. Nefedov, B. Orazsakhov, O.G. Ellert, A.A. Zharkikh, V.M. Novotortsev, A.I. Yanovsky and Yu.T. Struchkov, *J. Organomet. Chem.*, 444 (1993) 101.